BULLETIN OF MARINE SCIENCE, 66(2): 291–303, 2000

# TRANSPORT ACROSS THE WESTERN BOUNDARY OF FLORIDA BAY

*Ned P. Smith*

## ABSTRACT

Current meter time series, bottom pressure records and acoustic doppler profiler data assembled from three field studies conducted from 1994 to 1997 are combined with wind data to investigate the transport of water across the open western boundary of Florida Bay. Calculations suggest that the interaction of tidal variations in currents and water levels along the 81°05′W meridian transports water into Florida Bay at an average rate of 1470 $m^3 s^{-1}$. Fortnightly tidal cycles produce variations ranging from 35–150% about the mean. At a rate of 1470 $m^3 s^{-1}$, water level in the 2219 $km^2$ area east of the 81°05′W meridian would rise at a rate of 5.7 cm $d^{-1}$. It is hypothesized that Gulf water enters the bay faster than it can drain into Hawk Channel on the Atlantic side of the keys, and that outflow occurs also as a quasi-steady southwestward transport from the southern part of the bay, where tide-induced residual transport is weakest. Transport calculations indicate a region of weak but persistent outflow through the southern end of the boundary. Wind stress is coherent with flow across the western boundary primarily over time scales longer than seven days. Year-to-year differences in wind forcing are consistent with differences in net eastward transport through the central and northern parts of the boundary.

Results of a growing number of circulation studies in Florida Bay have identified a quasi-steady movement of water through the major tidal channels that separate Gulf and Atlantic sides of the Keys, as well as through many of the channels that connect sub-basins in the interior of the bay (Smith, 1994, 1998). While regional forcing by the Loop Current, the Florida Current and atmospheric pressure gradients may be important, local wind forcing and a tide-induced residual transport may contribute as well. Observations suggest that water moves west-to-east through the bay, entering from the broad shelf of the Gulf of Mexico, and exits through tidal channels along the southeast and south sides of the bay. Wang (1998) documented the movement of water through southern Florida Bay by tracking drogues that were released along or near the western boundary. A modeling study by Wang et al. (1994) simulated transport in Florida Bay forced by damped tidal waves and suggested that a tide-induced set-up of 1–2 cm within the bay helps explain the observed outflow through the tidal channels. Long Key Channel and Channel Five appear to play a major role in draining water from Florida Bay east of the 81°05′W meridian.

This paper focuses on the movement of water across the open western boundary of the bay. The two primary objectives of the study are to show that the southern part of the western boundary is a region of outflow, and to estimate the rate at which water is forced into Florida Bay by tide-induced residual transport. It is hypothesized that the interaction of tidal currents and water level variations drives water eastward into the bay and produces not only the outflow through the major tidal channels along the south side of the bay, but also a region of outflow along the southern end of the western boundary. Observations that document total transport suggest that outflow occurs where tidal amplitudes are lowest.

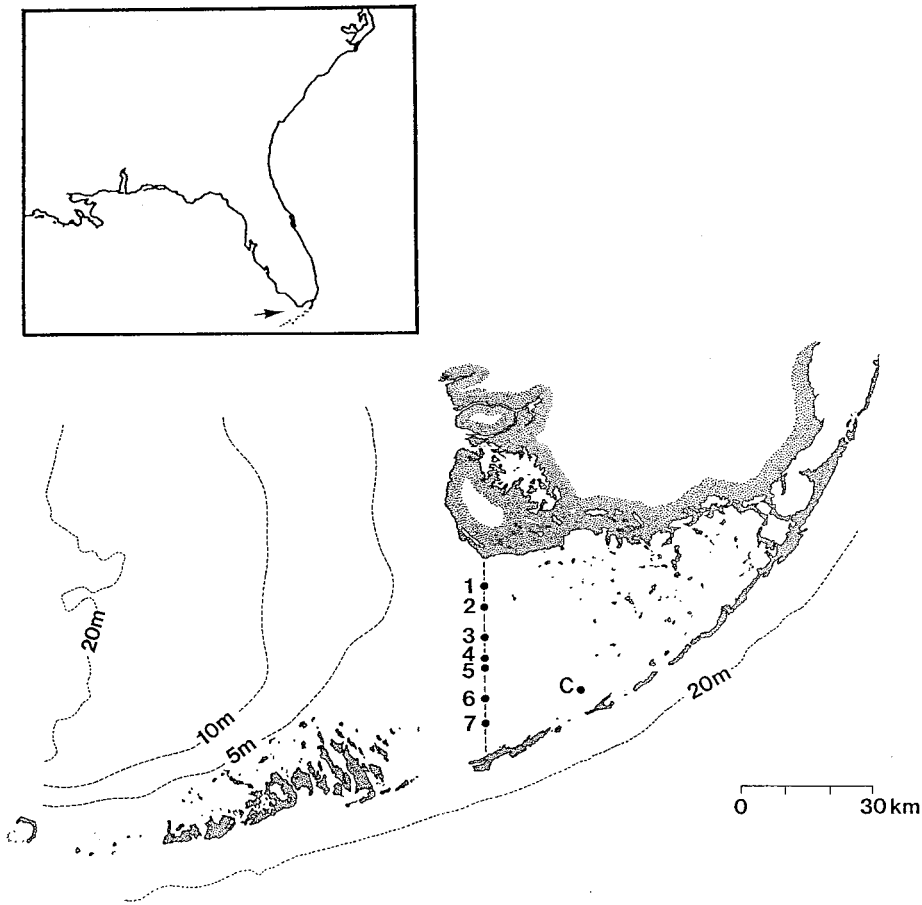


Figure 1. Map showing Stations 1–7 along the 81°05′W meridian, and the C-MAN weather station (indicated by C) in Florida Bay.

## DATA

The study area is the 81°05′W meridian, which is often taken to represent the western boundary of Florida Bay (Fig. 1). The distance from East Cape south to Marathon is 44.6 km, and the mean water depth is 3.0 m. Tidal amplitudes calculated from both current meter and water level records decrease from north to south (Smith, 1997).

Currentmeter data from three field studies involving seven study sites provide the basis for characterizing east-west flow across the western boundary of the bay. The first field study provided uninterrupted data from Stations 1 (25°05.0′N), 3 (24°57.5′N) and 6 (24°50.0′N), over the 274-d time period from 19 April 1994 to 17 January 1995. General Oceanics Mark II current meters were suspended from "gallows" type moorings and recorded the flow 1 m above the bottom. The speed and direction accuracy of the current meters is 1 cm $s^{-1}$ and 1°, respectively, according to the manufacturer's specifications.

Bottom pressure data were collected at the same three study sites, though for different periods of time. At the southern study site, a Brancker TG-205 in 3.4 m of water provided hourly data from 18 January to 4 April 1995. The accuracy of the TG-205 is ±2.1 cm. At

the central study site, a TG-205 in 3.9 m of water was in place from 2 May to 29 May 1995. At the northern study site, an Aanderaa WLR-5 in 3.2 m of water recorded bottom pressures from 21 September 1994 to 5 April 1995. The accuracy of the WLR-5 is ±1.4 cm.

Wind speed and direction, air temperature and surface pressure data were recorded during the first field study at the Coastal-Marine Automated Network (C-MAN) weather station near Long Key (indicated by "C" in Fig. 1). Wind speed and direction were recorded to the nearest 0.1 m $s^{-1}$ and 1°, respectively. Air temperature and air pressure, used to calculate air density, were recorded to the nearest 0.1°C and 0.1 mb, respectively.

In the second field study, SonTek Acoustic Doppler Profilers (ADP) were installed by the Army Corps of Engineers (WES) at Stations 1, 4 (24°55.0′N) and 7 (24°47.0′N). The speed and direction accuracy of the ADP are ±1% of the reading and ±1°, respectively (Slocum, 1999). A 266-d time period from 14 March to 5 December 1996 was selected for analysis. The southern WES study site was in 2.0 m of water, the central study site was in 2.8 m of water, and the northern study site was in 3.2 m of water. Currents above a 55-cm "blanking zone" were recorded in 4–12 layers, each with a thickness of 29 cm. The number of layers was determined by the mean depth and the tidal and nontidal rise and fall in sea level. Bottom pressures recorded by the ADP indicated water levels to the nearest 10 cm. Weather data from the C-MAN station were available only during the 151-d period from 2 July through 29 November 1996 to investigate wind forcing.

In the third field study, Stations 2 and 5 were maintained from 21 August to 20 November 1997, to improve spatial resolution for calculations of tide-induced residual transport. The southern study site was at 24°53.7′N in 3.4 m of water; the northern study site was at 25°01.3′N in 3.0 m of water. General Oceanics Mark II current meters recorded the flow 1 m above the bottom. Bottom pressure records are not available from the third study.

## Methodology

Two-dimensional Transport.—Vertically-integrated east-west transport, $T_{2D}$, in $m^2\ s^{-1}$, provided the basis for estimating tidal and total transport across the western boundary of Florida Bay at each study site. Transport, given by the product of the mean current speed and water depth, was calculated in either of two ways, depending on whether a current meter or a bottom-mounted ADP provided the data. When ADP measurements were used for the calculations, $T_{2D}$ was obtained from

$$T_{2D} = \sum_{i=1}^{n} u_i \Delta z, \qquad \text{Eq. 1}$$

where $u_i$ is the east-west component of the current in the ith layer, and $\Delta z$ is the layer thickness. A logarithmic current profile was assumed from the bottom up to the midpoint of the first level, 89 cm above the bottom. The current measured in the top layer was extrapolated upward when the pressure sensor indicated that a partial layer existed above the last full layer. Rounding errors that arise when ADP measurements are expressed to the nearest 10 cm will cancel over long periods, as overestimates are combined with underestimates. A discussion of errors associated with two-dimensional transport calculations is found in Appendix A.

When current meter data were used to estimate transport, upward and downward extrapolations of the east-west components assumed that the current profile was logarithmic. Integrating the east-west component of the current from surface to bottom, the instantaneous transport is given by

$$T_{2D} = \frac{u_*}{k}\left[ Z \log_e\left(\frac{Z}{z_0}\right) - \left(Z - z_o\right)\right], \qquad \text{Eq. 2}$$

where $u_*$ is the friction velocity, $k$ is the Kármán constant, $Z$ is the total water depth and $z_0$ is the roughness length (Smith 1994). The friction velocity was obtained from the expression for a logarithmic profile,

$$u(z) = \frac{u_*}{k} \log_e \left( \frac{z}{z_0} \right), \qquad \text{Eq. 3}$$

by substituting the measured current speed at the known height, $z$, above the bottom. A roughness length of 0.3 cm was used when the bottom was unvegetated (Heathershaw and Langhorne (1988). A value of 1 cm was used when the bottom was covered with seagrass. Smith (in press) used ADP profiles in an attempt to quantify the roughness length, but calculated $z_0$ values showed considerable scatter. It was concluded that without current measurements from the near-bottom blanking zone, where shear is greatest, it is better to estimate roughness lengths based on known bottom conditions. When water level measurements were not available, $Z$ was estimated as the sum of the mean depth and the predicted tide.

ADP profiles were used to test the validity of (3) for extrapolating mid-depth current measurements and using the extrapolated profile to estimate two-dimensional transport. To quantify differences between measured and extrapolated profiles, the second level of the ADP profile was taken to represent a current meter measurement, and current speed was extrapolated to the surface and bottom. At each level where the ADP profile provided a reading, the difference between observed and extrapolated speeds was calculated, and these values were used to obtain the mean difference and the standard error (Hoel, 1976).

THREE-DIMENSIONAL TIDAL TRANSPORT.—Only the tide-induced transport can be calculated simultaneously for the entire western boundary of the bay. Observations of currents and water levels were made at different times, and thus they cannot be combined to estimate the total transport. Harmonic analysis of time series of hourly water level and east-west current components identified the principal tidal constituents, and tide-induced residual transport was calculated using ten tidal constituents ($M_2$, $S_2$, $N_2$, $K_2$, $K_1$, $O_1$, $Q_1$, $P_1$, $M_4$ and $M_6$). All tidal constituents decreased in amplitude from north to south, and at the southernmost station amplitudes of several constituents were within the precision of the recording instrumentation. In general, $M_2$, $S_2$, $K_1$ and $O_1$ were the dominant constituents, while $Q_1$, $M_4$ and $M_6$ were small at all locations.

The calculation of tide-induced transport, in $m^3\ s^{-1}$, involves an interpolation of surface-to-bottom tidal transports calculated at the seven study sites. The 81°05′W meridian between East Cape and Marathon was sub-divided into seven segments, and the mean depth was determined for each segment. Surface-to-bottom transport was calculated from (2) using the east-west component of the predicted mid-depth tidal current and the sum of the mean depth and the predicted water level (Schureman 1958). The three-dimensional transport, $T_{3D}$, was calculated from the product of the two-dimensional transport and the segment width, $w$. $T_{3D}$ was reduced to zero at both ends of the 81°05′ meridian. There is no observational support for the rate at which east-west flow decreases near the northern or southern boundaries. To describe the current, a power law profile with an exponent of 0.125 was used. This confined most of the decrease in current speed to a region within 1 km of the coast. The tide-induced residual transport, $T_R$, was calculated by summing the hourly instantaneous transport measurements:

$$T_R = \sum_t \left[ \sum_{i=1}^{7} T_{2D,i} w_i \right] \Delta t, \qquad \text{Eq. 4}$$

Eastward flow into Florida Bay is defined to be positive. Summation over time of $T_{2D}$ without incorporating the segment width produces the cumulative east-west transport (see Figs. 3,4).

RESPONSE TO WIND FORCING.—Vertically-integrated east-west ADP transport past Stations 1, 4 and 7 using (1), and transport past Stations 1, 3 and 6 using (2) were paired with wind stress calculated from C-MAN weather observations in a spectral analysis (Little and Schure, 1988) to determine wind directions most effective in driving water into and out of the bay, and the time scales over which wind forcing is most important. Preliminary analyses using hourly east-west transport values indicated that highest coherences were confined to time scales longer than about 7 d. The longest

periodicity that could be resolved was 21 d. To focus specifically on longer time scales, all records were smoothed with a low-pass filter (Bloomfield, 1976) that removed 50% of the input variance at a period of 1.54 d (37 h).

## Results

Tidal Transport.—Figure 2 is a plot of the cumulative net east-west tide-induced residual transport across the western boundary of Florida Bay for one synodical month, 1–29 July 1998. The slope of the line indicates a mean inflow of 1610 $m^3 s^{-1}$. Deviations about the mean are significant. Neap tide conditions, probably combined with equatorial tide conditions, reduce the transport rate substantially. Low-pass filtered hourly values decrease to about 700 $m^3 s^{-1}$ during the first few days of the month, and to about 1250 $m^3 s^{-1}$ during 16–17 July. Conversely, spring tide conditions, possibly reinforced by tropic tide conditions, increase the rate to about 2225 $m^3 s^{-1}$ during 11–12 July and again during 23–24 July. A one-year simulation (not shown) which is less sensitive to the interaction of fortnightly cycles, indicates a mean inflow of 1470 $m^3 s^{-1}$. Minimum and maximum inflow rates commonly reach 600 and 2200 $m^3 s^{-1}$. Total flood tide volume transports vary from about 190–580 $\times 10^6$ $m^3$, and total ebb tide volume transports vary from about 100–550 $\times 10^6$ $m^3$. The surface area of the bay east of the 81°05′W meridian is 2219 $km^2$. Inflow at a rate of 1470 $m^3 s^{-1}$ would raise the water level at a rate of 5.7 cm $d^{-1}$.

Two additional synodic-month simulations represented transport across the western boundary of the bay during October and February. At these times of year, seasonal variations in sea level raise and lower water levels +9.5 and -10.0 cm, respectively (Smith, 1997). The October inflow rate is approximately 0.5% greater than the July rate, and the February rate is approximately 0.5% lower. Thus, the seasonal rise and fall in sea level has a minimal effect on the mean tide-induced residual transport. Two final simulations explored the effect of wind-forced variations in sea level. The set-up and set-down of

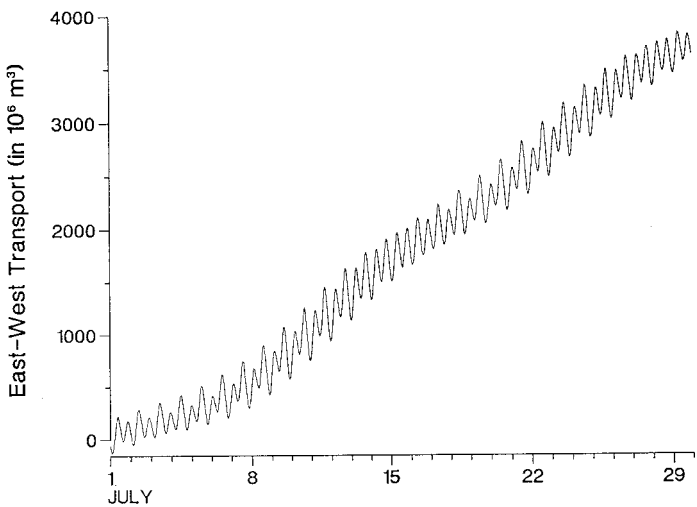


Figure 2. Cumulative net tide-induced volume transport (in millions of $m^3$) through the western boundary of Florida Bay, 1–29 July 1998. Calculated with ten diurnal, semidiurnal and shallow-water tidal constituents. Increasingly positive transport indicates flow into Florida Bay.

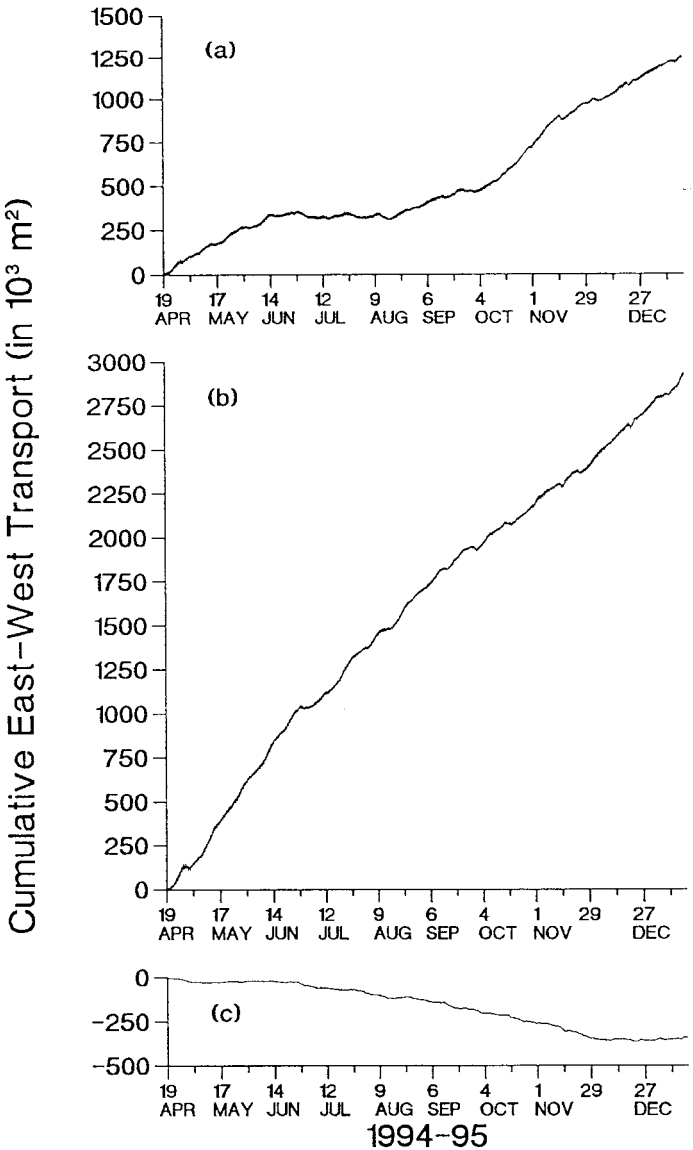


Figure 3. Two-dimensional, surface-to-bottom cumulative net total transport past Station 1 (a), Station 3 (b) and Station 6 (c), 19 April 1994 through 17 January 1995 (first field study). Positive transport indicates flow into Florida Bay.

water level in Florida Bay can be on the order of 20–30 cm, (Smith and Pitts, 1995). The effect on tide-induced residual transport of changing the mean water depth by ±25 cm was ±1.4%.

The importance of individual tidal constituents in moving water across the western boundary of the bay was determined from (4) by accumulating transport over flood and ebb half tidal cycles. $T_{3D}$ was calculated and summed with 60-s time steps. Asymmetry in tidal transport is greatest for the $M_2$ constituent. East-west transport at peak $M_2$ flood and ebb are 27.0 and $-22.1 \times 10^3$ m$^3$ s$^{-1}$. Summing inflow and outflow from one slack water to

the next, the amount of water moving across the western boundary on the flood and ebb are 375.2 and $-319.9 \times 10^6$ m$^3$, respectively. Asymmetry in the other constituents results in flood transports 3–6% greater than ebb transports. Transport totals are 74.7 and $-71.6 \times 10^6$ m$^3$ for the $S_2$ constituent, 124.6 and $-118.0 \times 10^6$ m$^3$ for the $K_1$ constituent, and 97.6 and $-95.1 \times 10^3$ m$^3$ s$^{-1}$ for the $O_1$ constituent.

TOTAL TRANSPORT.—Current meter measurements made at Stations 1, 3 and 6 in the first field study, and ADP profiles from Stations 1, 4 and 7 in the second field study were used to calculate cumulative total east-west transport. These measurements contain both tidal and nontidal components, thus results are distinctly different from those obtained from tidal predictions. Because results are specific to the time period over which data were recorded, and because the data used here are from two field studies, all the time series cannot be combined to estimate the total transport into or out of the bay. Due to the relatively poor station spacing, no attempt was made to interpolate along the 81°05' meridian to estimate total volume transport from either the 1994–95 or the 1996 data alone.

Figure 3 is a plot of cumulative east-west transport past Stations 1, 3 and 6, using the current meter data obtained from the 1994–95 field study. Positive values indicate a net transport of water eastward into Florida Bay. Results indicate an inflow at the northern and especially the central station, but a weak outflow at the southern station. At the central station, with a mean depth of 3.9 m, the cumulative net transport of $2919 \times 10^3$ m$^2$ over the 6576-h study corresponds to a depth-averaged inflow of 3.2 cm s$^{-1}$. Similar calculations indicate a depth-averaged inflow of 1.4 cm s$^{-1}$ at the northern station and an outflow of −0.5 cm s$^{-1}$ at the southern station.

Figure 4 is the east-west component of the total transport of water past Stations 1, 4 and 7, using ADP profiles from the 1996 field study. Results are qualitatively similar to those obtained from the first field study, although the magnitude of the inflow is quite different at the central station. The net transport at the northern and central stations is into the bay, and again the southern study site is in a region of outflow. Average depth-integrated east-west current speeds are +2.3, +1.0 and −0.9 cm s$^{-1}$, for the northern, central and southern stations, respectively.

When ADP profiles were compared with logarithmic profiles extrapolated vertically from the second level in the ADP profile, standard errors of the differences suggested that the instantaneous current profile can deviate significantly from a logarithmic profile, but that the deviations largely cancel over long time periods. One thousand observed and extrapolated profiles were compared at each of the three stations. Although profiles closely approximated logarithmic profiles in some cases, the match was poor in others. Standard errors of 3–4 cm s$^{-1}$ were most common, occurring 19% of the time at Station 1 and 28% of the time at both Stations 4 and 7. An encouraging result, was the tendency of differences to cancel over longer periods of time. For example, the average error calculated from 1000 observed-calculated current speed differences at the top level at Station 1 was −0.86 cm s$^{-1}$, and the error decreased to −0.16 cm s$^{-1}$ in the third layer below the surface. The tendency for observed east-west flow to be more westward than calculated east-west flow is interpreted as an effect of the net westward-directed wind stress during the same time period. Average top-level errors at Stations 4 and 7 were −0.13 and −0.47 cm s$^{-1}$, respectively. All these values are within the accuracy of the current meter.

WIND FORCING.—Spectral analyses of low-pass filtered wind stress components and the east-west transport revealed both similarities and differences in the response to wind forcing along the western boundary of the bay. Results are summarized in Table 1. In all

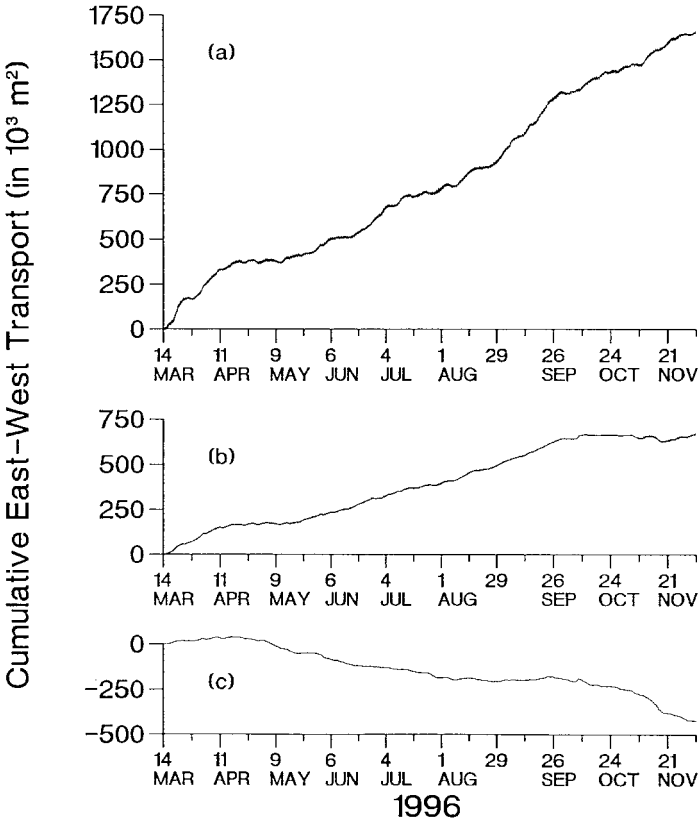


Figure 4. Same as Figure 3, but for Station 1 (a), Station 4 (b) and Station 7 (c), 14 March through 4 December 1996 (second field study).

cases, highest coherences were found for time scales longer than about 7 d, where energy density levels are highest. In both field studies, northwestward wind stress was most effective in forcing water across the northern part of the western boundary, while southwestward wind stress was most coherent with east-west transport through the southern part of the boundary. East-west flow past Station 1 is constrained topographically by East Cape and the western extension of First National Bank. South of about Station 3, the flow is less affected by nearby land boundaries. Coherence levels are lower at all three study sites in the first field study, perhaps because near-surface currents most influenced by the wind were extrapolated from mid-depth measurements rather than measured directly. The lowest and highest coherences were found at the two southernmost stations. The lowest value appeared at Station 6, where surface currents were extrapolated from mid-depth measurements. The highest value was obtained at Station 7, where surface currents were measured at the top of the ADP profile.

Resultant wind stress vectors during the two field studies were nearly identical in direction, but they differed somewhat in magnitude. The resultant magnitude and direction for the first study were 0.291 dyne $cm^{-2}$ and 269°. For the second field study, the resultant direction was 267°, but the magnitude of the resultant wind stress was 0.357 dyne $cm^{-2}$,

Table 1. Wind stress components, Φ, most coherent with east-west transport across the western boundary of Florida Bay, and highest coherence values, $C_{max}$ within the 7–21 day period range.

| | | Φ | $C_{max}$ |
|---|---|---|---|
| a. First Field Study | | | |
| | 1. Station 1 | 155–335° | 0.67 |
| | 2. Station 3 | 115–295° | 0.65 |
| | 3. Station 6 | 055–235° | 0.53 |
| b. Second Field Study | | | |
| | 1. Station 1 | 135–315° | 0.73 |
| | 2. Station 4 | 075–255° | 0.76 |
| | 3. Station 7 | 060–240° | 0.88 |

which is 23% larger than that found for the first field study. The resultant wind stress was favorable for forcing water through the central part of the western boundary, and to a slightly lesser extent through the southern part of the boundary. Resultant winds were least favorable for forcing water out through the northern part of the boundary.

## Discussion

The comparison of east-west transport calculated from bottom pressures and mid-depth currents in the first study with transport calculated from ADP data in the second study reveals both similarities and differences. Similarities are in the form of general patterns of inflow and outflow. In both field studies, the northern two-thirds of the western boundary of the bay appears to be a region of inflow, while the southern third emerges as a region of weak outflow. The westward flow from the southern part of Florida Bay is a logical consequence of the north-to-south decrease in tidal amplitudes (Smith, 1997) and the clockwise rotation of tidal ellipses to an orientation that more nearly parallels the 81°05′ meridian (Smith and Pitts, 1995), both of which would make tide-induced residual inflow less effective.

The primary difference is in the region of strongest inflow. Results from the first field study suggest that inflow is strongest through the middle of the western boundary (Fig. 3B), while results from the second study suggest that inflow is strongest just south of East Cape (Fig. 4A). The difference between part (b) of Figure 3 and part (b) of Figure 4 may be a result of the nearly 5 km distance between Stations 3 and 4. North-south differences in long-term net east-west flow over distances of a few kilometers could not be resolved from these studies. Differences between the 1994–95 and 1996 inflow at Station 1 (Figs. 3A,4A) and at Stations 3 and 4 (Figs. 3B, 4B) are in agreement with differences in wind forcing, however. In both years, resultant wind stress was favorable for forcing water out of the bay through the central part of the western boundary, but the significantly weaker inflow calculated for Station 4 in 1996 is consistent with the stronger westward wind stress during the 1996 field study. The cause of the stronger inflow past Station 1 in 1996 is less clear. Resultant wind stress was not in a direction favorable for forcing water out of the bay at that location during either year. Westward wind stress can produce a set-down of water level in the bay, however (Smith, in press). Thus, the stronger inflow at Station 1 may reflect the indirect effects of stronger wind forcing in the form of an enhanced eastward directed barotropic pressure gradient.

Seasonal variations in winds over the Florida Keys (NOAA, 1998a,b) include winds out of the southeast and east-southeast from February through September, and out of the north-northeastern quadrant from October through January. This suggests a seasonal cycle in wind forcing through the western boundary of the bay. During summer months, wind stress into the northwestward quadrant would act to inhibit inflow through the northern part of the boundary and encourage inflow through the central part. Similarly, during winter months, wind stress directed into the south-southwestward quadrant would encourage outflow through the central and southern parts of the boundary and thus encourage inflow through the northern part.

The net eastward transport of water is only one of two important tide-related transport processes that can impact Florida Bay. The oscillatory ebb and flood of the tide across the open western boundary can be significant also, even if there is no net volume transport. The net exchange of bay and shelf waters through turbulent mixing could not be determined, but some fraction of the shelf water entering on the flood must remain in the bay, and similarly some fraction of bay water must remain in the Gulf following each ebb. Even if only 3.5% of the water leaving through the western boundary on an average ebb tide remains in the Gulf, the loss of Florida Bay water by tidal mixing would be equivalent to the loss of bay water through Long Key Channel during each $M_2$ tidal cycle.

Results from earlier studies (Smith, 1998) suggest that a tide-induced residual transport through all the major tidal channels along the southeast side of the bay reinforces the tide-induced residual inflow through the open western boundary and contributes to the set-up of water levels in the interior of the bay. For example, tide-induced residual transports through Channel Two and Channel Five are inflows of 69 and 100 $m^3\ s^{-1}$, respectively. Unpublished data from Long Key Channel indicate tide-induced transport of 157 $m^3\ s^{-1}$. The combined tide-induced residual inflow through the tidal channels is about 20% of the inflow calculated for the western boundary of the bay. In all channels, however, the effect of the local tide-induced residual transport is reversed, apparently by the set-up of water within the bay, and the total residual transport is an outflow into Hawk Channel. Unpublished data from Channel Five indicate a net outflow of 190 $m^3\ s^{-1}$ during a 38-d time period in 1990, and outflow through Channel Two was 54 $m^3\ s^{-1}$ during an equally short study period. A 385-d study conducted in 1992–93 indicated a mean outflow of 260 $m^3\ s^{-1}$ (Smith, 1994). The paradigm suggested by these observations is that the tide-induced transport of water into the bay through the western boundary and through tidal channels is of sufficient magnitude to raise water levels in the bay and maintain an outflow through the same tidal channels and through the southern part of the western boundary.

## Acknowledgments

The assistance of P. A. Pitts in the field work and preliminary reduction of the data is greatly appreciated. Support for the first field study was from the Florida Department of Environmental Protection under Agreement MR020. Data from the second field study were collected by the U.S. Army Corps of Engineers, Waterways Experiment Station; support for the analysis of the data was provided through contract number DACW17-96-M-0420. Support for the third field study was from the NOAA Coastal Program through contract number NA 76RGO480.

## Literature Cited

Bloomfield, P. 1976. Fourier analysis of time series: an introduction. John Wiley & Sons, New York. 258 p.

Dennis, R. E. and E. Long. 1971. A user's guide to a computer program for harmonic analysis of data at tidal frequencies. NOAA Tech. Rpt. 41, U.S. Dept. Comm., Rockville, Maryland. 31 p.

Eisensmith, S. 1985. PlotIT Interactive Graphics and Statistics, Version 1.0 Scientific Programming Enterprises. Haslett, Minnesota.

Heathershaw, A. D. and D. N. Langhorne. 1988. Observations of near-bed velocity profiles and seabed roughness in tidal currents flowing over sandy gravels. Estuar. Coast. Shelf Sci. 26: 459–482.

Hoel, P. G. 1976. Elementary Statistics, 4th ed. John Wiley & Sons, New York, 361 p.

Little, J. N. and L. Schure. 1988. Signal Processing Toolbox for use with Matlab. The MathWorks, Inc., Natick, Massachusetts.

National Oceanic and Atmospheric Administration. 1998a. Local climatological data, annual summary with comparative data, Key West, Florida. National Climatic Data Center, Asheville, North Carolina.

_____. 1998b. Local climatological data, annual summary with comparative data, Miami, Florida. National Climatic Data Center, Asheville, North Carolina.

Schureman, P. 1958. Manual of harmonic analysis and prediction of tides. Spec. Publ. No. 98, rev. ed., U.S. Govt. Printing Office, Washington, D.C. 317 p.

Slocum, D. B. 1999. Sontek, 7966 Arjons Drive, Suite D, San Diego, California 92126. Pers. Comm.

Smith, N. P. 1994. Long-term Gulf-to-Atlantic transport through tidal channels in the Florida Keys. Bull. Mar. Sci. 54: 602–609.

_____. 1995. Observations of steady and seasonal salt, heat and mass transport through a tidal channel. J. Geophys. Res. 100: 13,713–13,718.

_____. 1997. An introduction to the tides of Florida Bay. Fla. Sci. 60: 53–67.

_____. 1998. Tidal and long-term exchanges through channels in the Middle and Upper Florida Keys. Bull. Mar. Sci. 62: 215–227.

_____. (in press). Observations of shallow-water transport and shear in western Florida Bay. J. Phys. Oceanogr.

_____ and P. A. Pitts. 1995. Low-frequency tidal and seasonal water level variations in Florida Bay. Final Rpt., Coop. Agreement CA 5280-4-9022. Harbor Branch Oceanographic Institution, Fort Pierce, Forida. 52 p.

Wang, J. A. 1998. Subtidal flow patterns in western Florida Bay. Estuar. Coast. Shelf Sci. 46:901-915.

Wang, J. D., J. van de Kreeke, N. Krishnan and D. Smith. 1994. Wind and tide response in Florida Bay. Bull. Mar. Sci. 54: 579–601.

Date Submitted: September 2, 1998. Date Accepted: October 22, 1999.

Address: *Harbor Branch Oceanographic Institution, 5600 U.S. Highway 1 North, Fort Pierce, Florida 34946*

## Appendix A. Error Analysis

1. Instrument Errors.—Errors in two-dimensional transport calculations can arise from inaccuracies of current and bottom pressure measurements. Maximum errors that could be attributed to instrumentation accuracy were quantified by recalculating transport at Station 1 with current speeds increased and decreased by 1 cm $s^{-1}$, current directions

changed by ±1° and water levels increased and decreased by 1.4 cm. Results indicate that the accuracy of the current meter is more important than the accuracy of the pressure recorder. Changes in water depth alone increased and decreased total transport by about 0.2%. Total transport increased by about 4% when both current speeds and water levels were increased. Values decreased by the same amount when current speeds and water levels were decreased. Tidal transport across the western boundary is affected less because only part of the measured current is tidal, and the flood and ebb may not be in an east-west direction. When accuracies were applied to tide-induced residual transport calculations for Station 1, transport varied by ±3.5%.

2. Uncertainty in Harmonic Constants.—Errors in estimates of tide-induced residual transport can arise from uncertainty surrounding the amplitudes and local phase angles used in the calculations. When current meter and bottom pressure records are substantially longer than the 29-d time periods needed for a single harmonic analysis (Dennis and Long, 1971), multiple harmonic analyses gave several amplitude and phase angle pairs for each of the 10 tidal constituents. Individual amplitude and phase angle pairs were then vector-averaged, and resultant values were used in the calculations. The individual pairs, however, can be used also to quantify scatter about the vector averages. To quantify the scatter in amplitude, the deviation of each amplitude from the vector mean amplitude was expressed as a percent of the vector mean and plotted against the vector mean amplitude. To quantify the scatter in phase angle, the average deviation from the vector mean, in degrees, was calculated and plotted as a function of the vector mean amplitude. This approach maintained a distinction between scatter in amplitude and scatter in phase angle when one is relatively large and the other is relatively small.

For both amplitudes and phase angles, scatter was greatest for the low-amplitude tidal constituents, and it decreased quickly as the vector-mean amplitude increased. A curve-fitting program (Eisensmith, 1985) was used to describe the decrease in scatter with increasing amplitude. An exponential decrease was assumed for both currents and water levels. For water levels, the scatter in amplitude, $S_a$, and phase angle, $S_p$, for the $j^{th}$ tidal constituent can be expressed as a function of its vector-averaged amplitude, A, with

$$S_a = \pm 11.5\% \exp(-0.62\, A_j), \text{ and } S_p = \pm 7.2^{o} \exp(-0.051\, A_j), \qquad \text{Eq. 5}$$

respectively. Thus, for example, the scatter about the vector-average phase angle was on the order of ±7° about the mean if the amplitude of the constituent was very low, but it decreased to less than 1° for the largest amplitude of nearly 40 cm. Similarly, for current meter data, the scatter of the amplitude and phase angle are given by

$$S_a = \pm 16.0\% \exp(-0.066\, A_j), \text{ and } S_p = \pm 6.1^{o} \exp(-0.026\, A_j), \qquad \text{Eq. 6}$$

respectively. While 11–16% and 6–7° represent considerable uncertainty, this degree of scatter applies only to the very low-amplitude constituents, and they in turn are responsible for a small fraction of the total transport.

To characterize the effect that uncertainty in amplitudes and phase angles might have on transport calculations, transport was recalculated as phase angles were alternately lagged and advanced, and as amplitudes were alternately amplified and reduced. Changes involved all ten constituents for water levels or currents simultaneously, and constituents were not adjusted individually. For each permutation, the result was compared to the tide-

induced residual transport obtained when vector-averaged harmonic constants were used. Transport increased by 7.5% when amplitudes were increased for both water levels and currents, phase angles for water levels were lagged and phase angles for currents were advanced. Transport decreased by a similar amount when amplitudes were reduced for both water levels and currents, phase angles for water levels were advanced and phase angles for currents were lagged.

3. Tidal Predictions.—An additional source of errors arises when water level records are not available to provide hourly values of $Z$, and the water depth is approximated by the sum of the mean water depth and the predicted tide. Calculations of total transport for a 190-d period when water level measurements were available from Station 1, and for a 48-d period when water level measurements were available from Station 6, indicated that transport calculated using the mean water level and tidal predictions is a close approximation to transport calculated using water level observations. At Station 1, transport calculated from predicted tides superimposed onto the mean water level was 97.9% of transport calculated with bottom pressure records. At Station 6, transport calculated with predicted tides was 103.5% of transport calculated with bottom pressure records. Similar findings from an earlier study (Smith, 1995) suggest that low-frequency fluctuations in currents and water level are poorly correlated and thus contribute little to the tide-induced residual transport.